Electronic Supplementary Material (ESI) for ChemComm.

Supplementary information

Low molecular weight and highly functional RCF lignin products as a full bisphenol A replacer in bio-based epoxy resins

Korneel Van Aelst, Elien Van Sinay, Thijs Vangeel, Yingtuan Zhang, Tom Renders, Sander Van den Bosch, Joost Van Aelst, Bert F. Sels*

Center for Sustainable Catalysis and Engineering, KU Leuven, Celestijnenlaan 200 F, 3001 Leuven, Belgium

* corresponding author, e-mail: bert.sels@kuleuven.be

Table of Contents

1. Experimental procedures

A. Chemicals and materials

All commercial chemicals were analytic reagents and were used without further purifications. 5 % Ru on Carbon (Ru/C), tetrahydrofuran (>99%, stabilized with 250 ppm BHT), dmso-d_6 (99.9 % atom D), 2-chloro-4,4,5,5-tetramethyl-1,3,2-dioxaphospholane (95%), chromium (III) acetylacetonate (97%), cholesterol (99%), choroform-d (99.8% atom D), tetrabutylammonium bromide (TBAB), epichlorohydrin (99%), sodium hydroxide, magnesium sulfate, 3,5-dimethoxy-4-hydroxybenzaldehyde, 3-phenyl-1-propanol, 4-propylguaiacol, Bisphenol A diglycidyl ether (>98%) and anhydrous pyridine (99.8%) were purchased from Sigma Aldrich. n-heptane (>99%), ethyl acetate (99.5%), and methanol (99.9%) were purchased from Acros organics. Dichloromethane (>99%) was purchased from Fischer Chemical Ltd. Pine was obtained from a local dealer (Aveve).

B. Reductive Catalytic Fractionation

The RCF experiment was performed in a 2 L stainless steel batch reactor (Parr Instruments & Co.). 150 g of pine was loaded into the reactor, together with 15.0 g Ru/C and 800 mL methanol. Subsequently, the reactor was sealed, flushed three times with N_2 (10 bar) and then pressurized with H_2 (30 bar at room temperature). Next, the reaction mixture was stirred (750 rpm) and simultaneously heated to 235 °C (~30 min. heating time). After the reaction time of 3h, the reactor was cooled and depressurized at room temperature. The reactor contents were quantitatively collected by washing the reactor with ethanol.

The solid pulp was separated by filtration and washed thoroughly with acetone. Next, the resulting filtrate was evaporated and a brown oil was obtained, which was subjected to a threefold liquid-liquid extraction using dichloromethane (DCM) and water. To obtain the RCF lignin oil, the DCM-extracted phase was dried in an oven of 80 °C.

C. Fractionation

The RCF lignin oil was fractionated using a sequential extraction protocol. Approximately 15 g of lignin was threefold extracted at 80 °C for 0.5 h with 75 mL of heptane. The soluble phase was decanted and the resulting heptane residue (P_1) was dried by rotary evaporation. Subsequently, a fractionation based on solvent-anti-solvent precipitation was used to separate this heptane residue in 4 fractions (F_1-F_4). Therefore, 6 g of the residue was solubilized in 30 mL ethyl acetate (solvent). Next, 10 mL of heptane (anti-solvent) was added to this mixture to obtain a binary solvent mixture containing 75 volume % ethyl

acetate and 25 volume % heptane (Figure S1). A cloudy mixture was formed and by centrifugation (10 minutes, 1000 rpm) a clear soluble mixture and a precipitate was formed. The precipitate (F1) was dried in an oven of 80 °C, and the soluble mixture was transferred to a second recipient. More heptane was added to this mixture to obtain a binary solvent mixture containing 50 volume % ethyl acetate and 50 volume % heptane and the previous steps were repeated. In the end, by following this approach, four different fractions were obtained:

(i) F_1: precipitate in 75 volume % ethyl acetate / 25 volume % heptane

(ii) F_2: precipitate in 50 volume % ethylacetate / 50 volume % heptane

(iii) F_3: precipitate in 25 volume % ethylacetate / 75 volume % heptane

(iv) F_4: soluble fraction in 25 volume % ethylacetate / 75 volume % heptane

D. **GPC analysis**

The distribution of the molar mass of the lignin products was investigated using gel permeation chromatography – size exclusion (GPC-SEC). Therefore, a lignin sample was solubilized in THF (5 mg mL^{-1}) and subsequently filtered with a 0.2 µm PTFE membrane to remove any particulate matter to prevent plugging of the column. GPC-SEC analyses were performed at 40 °C on a Waters E2695 equipped with a PL-Gel 3 µm Mixed-E column with at length of 300 mm, using THF as a solvent with a flow of 1 mL min^{-1}. The detection was UV based at a wavelength of 280 nm. Calibration were based on calibration with commercial polystyrene standards of Agilent.

E. ^{1}H-^{13}C HSQC spectroscopy

Approximately 70 mg of the lignin sample was dissolved in 0.6 mL DMSO-d_6 and loaded in an NMR tube. The two-dimensional ^{1}H-^{13}C HSQC spectroscopy experiment was conducted at 298K using a Bruker Avance III HD 400 MHz console with a Bruker Ascend™ 400 Magnet, equipped with a 5 mm PABBO probe. A Bruker standard pulse sequence ('hsqcedetgp') was used for semi-quantification with the following parameters: spectral width in F2 dimension (^{1}H) of 13 ppm using 2048 data points, a spectral width in F1 dimension (^{13}C) of 165 ppm, using 256 data points, a total of 8 or 16 scans were recorded with a 2s interscan delay (D1). Topspin 4.0.2 software was used for data processing and volume integration. The spectra was processed in 2048 data points in the F2 and F1 dimension (with one level of linear prediction and 32 coefficients). The solvent peak of DMSO was used as the internal reference (δ_c/ δ_H: 39.5 ppm/2.49 ppm) following by manually phasing and automatic baseline correction.

F. ^{31}P-NMR analysis

^{31}P-NMR measurements were performed using a standard phosphitylation procedure.[1] A solvent solution (1.6 pyridine : 1 $CDCl_3$) was used to make stock solutions of the internal standard (cholesterol, 20 mg mL^{-1}) and relaxation agent (chromium acetylacetonate, 10 mg mL^{-1}). An amount of lignin (approximately 20 mg) was accurately weighed and 100 µL of the internal standard solution and 50 µL of the relaxation agent solution was added, next to 400 µL of solvent solution. Subsequently, 75 µL of 2-chloro-4,4,5,5-tetramethyl-,1,3,2-dioxaphospholane (TMDP) was added and the sample was thoroughly mixed before transferring them to the NMR-tube. ^{31}P-NMR spectra were obtained on a Bruker Avance III 400 MHz NMR using a standard phosphorous pulse program (256 scans, 5s interscan delay, O1P 140 ppm). The chemical shifts were calibrated by assigning the sharp peak of residual water + TMDP at 132.2 ppm and automatic baseline correction was applied.

G. Glycidylation procedure

Approximately 300 mg of lignin was loaded in a round bottom flask, together with TBAB (0.1 eq *vs* number of phenolics) and epichlorohydrin (20 eq. *vs* number of phenolics). This mixture was stirred and heated to 85 °C for 5 h. Afterwards, the flask was rapidly cooled in an ice bath and a concentrated solution of NaOH was added dropwise (3 eq. *vs* number of phenolics). This reaction was continued for 3 h at room temperature. After the reaction, 20 mL of ethyl acetate and 20 mL water was added to extract the organic phase from the salts and TBAB. The ethyl acetate phase was washed 3 times with an additionally 20 mL of water, dried with magnesium sulfate and filtered over a Whatman grade 5 filter. Next, the epichlorohydrin and ethyl acetate was removed by rotary vacuum evaporation

H. Determination of EEW

To obtain the EEW, the samples were analysed by ^{1}H-NMR. To approximately 30 mg of sample (carefully weighed), 5 mg of internal standard (3,5-dimethoxy-4-hydroxybenzaldehyde) was added next to 600 µL $CDCl_3$. The signal according to the CH_2 of the oxirane group was integrated relative to the internal standard. Since these signals overlap with lignin signals, this relative value was corrected to a blanc sample (the non-glycidylated lignin fraction).

I. Thermal curing with amine

Diethylenetriamine (DETA) was used a crosslinking agent for the lignin-based pre-polymers. DETA and the lignin fraction were solubilized in little acetone to improve their mixing in a Teflon mold. Next, the solvent was gradually removed and the epoxy resin was formed by following temperature program: 2 h at 45 °C, 2 h at 60 °C, 1 h at 70 °C, 1h at 80 °C and 2 h at 140 °C.

J. Thermal analysis

Thermogravimetrical analysis of the cured resins was performed while heating under N_2 using a TA instruments TGA Q500. About 10 mg of the dried sample was heated at 10 °C min^{-1} to 575 °C at a flow rate of 20 mL min^{-1}. TGA allows determination of the degradation temperature and simultaneously indicated the absence of residual solvents. Differential Scanning Calorimetry (DSC) measurements were performed on a DSC Q2000 (TA Instruments) by cycling between 20 and 200 °C with heating/cooling rates of 10 °C min^{-1}. The second heating cycle was used to determine the Tg.

K. ATR-FTIR spectroscopy

FT-IR spectra were acquired in vacuo on a Bruker IFS 66 v/s Vacuüm FTIR spectrophotometer. The samples were measured using 32 scans with a resolution of 4 cm^{-1} and corrected relative to a blanc. The lignin fractions and glycidylated fractions were measured in ATR-FT-IR mode, the resins were measured using the KBr method.

2. Supplementary notes

A. Supplementary note 1

Unique and valuable lignin streams can be obtained in a *lignin*-first biorefinery. Here, the primary focus is on lignin extraction and exploitation, still producing a carbohydrate fraction useful for the production of chemicals and materials.[2] Besides lignin protection concepts, one emerging *lignin*-first biorefinery is Reductive Catalytic Fractionation (RCF). RCF effectuates the extraction of lignin from the lignocellulosic biomass, as well as its *in* situ depolymerization and reductive, metal catalyzed stabilization of the resulting lignin fragments. This final step is key, since it prevents the C-C condensation of lignin, occurring in traditional biorefineries. Besides, proper choice of the metal catalyst allows to tune the desired functionality of the resulting lignin fraction. This stabilizing strategy enables the production of a low molecular weight lignin stream (*i.e.* monomers and small *oligomers)* and a carbohydrate rich pulp.[3]

In this study, non-extracted pine wood was processed under benchmark RCF conditions at the 2 L scale. Therefore, 150 g of pine, 15 g of Ru/C and 800 mL methanol were added to a 2 L Parr batch reactor. The mixture was pressurized with hydrogen (30 bar at room temperature), stirred at 600 rpm and heated to 235 °C for a reaction time of 3 h. After cooling, filtration, methanol evaporation and DCM-water extraction, a stable, low molecular weight lignin oil was obtained, representing 16.3 wt% of the original biomass weight. This lignin oil (F_{oil}) contains 25.9 wt% phenolic monomers and has a M_n of 444 g mol^{-1}.

The combination of the large content of phenolic monomers and the low molecular weight is not desirable to produce epoxy resins, since at least 2 oxirane moieties per molecule are necessary to provide proper crosslinking in the cured polymer. Therefore, most of the phenolic monomers are removed by an easy heptane extraction, resulting in two fractions: (i) the heptane soluble fraction (F_{hept}) with a M_n of 224 g mol^{-1} and (ii) the heptane insoluble fraction (P_1) with a M_n of 703 g mol^{-1} (Figure S5). This heptane soluble fraction has been demonstrated to be useful for a variety of applications such as the production of phenol or safer, renewable bisphenols.

B. Supplementary note 2

To study the impact of the molecular weight, P_1 was fractionated by using an easy sequential solvent-anti-solvent precipitation. P_1 was fully soluble in ethyl acetate (solvent), yet addition of heptane (anti-solvent) resulted in a precipitate, which could be decanted after centrifugation from the soluble fraction. Subsequent addition of heptane to the latter fraction resulted in a second precipitate and a second soluble fraction. By using this approach, 4 fractions were obtained: (i) F_1 (precipitate in 75 vol% EtoAc/25 vol% heptane), (ii) F_2 (precipitate in 50 vol% EtoAc/50 vol% heptane), (iii) F_3 (precipitate in 25 vol% EtoAc/75 vol% heptane), (iv) F_4 soluble fraction of 25 vol% EtoAc/75 vol% heptane). These resulting 5 fractions were thoroughly characterized before glycidylation and thermal curing.

C. Supplementary note 3

Cleavage of the β-O-4 inter-unit linkage and reductive stabilization of the intermediates is proven by the near absence of the β-O-4 inter-unit linkage and the high number of end-units – the reaction products – in all fractions (Table S1). Overall, the relative number of end-units decreases with increasing molecular weight of the RCF oligomers, since the number of phenolics per molecule and thus the amount of inter-unit linkages increases. Predominantly two types of end-units can be found: 4-propanol (4-POH) and 4-propyl. Interestingly, their relative abundance varies, since relatively more 4-POH to 4-P can be found in higher molecular weight fractions. Effective cleavage of the ether structure in native C-C inter-unit linkages such as β-5 phenylcoumaran, β-β resinol, and β-1 spirodienone is also proven, since none of these native ether linkages can be detected in the ^{1}H-^{13}C HSQC spectra (Table S1). β-5 phenylcoumaran is selectively converted to β-5 γ-OH and β-5 E. Their relative abundance (β-5 E to β-5 γ-OH) decreases with increasing molecular weight. Thus, a higher number of polar aliphatic hydroxyl groups can be found on the β-5 linkages of higher molecular weight RCF oligomers. Similar trends can be observed for the products resulting from the hydrogenolysis of β-1 spirodienone: β-1 γ-OH and β-1 E, and the products resulting from the hydrogenolysis of β-β resinol: β-β 2x γ-OH and β-β THF. Presumably, this is due to a combined effect of polarity - and thus solubility – differences, and differences in chemical reactivity between lower and higher molecular weight oligomers.

D. Supplementary note 4

a. Optimization of glycidylation

When performing a glycidylation reaction, two main possible side reactions can occur: (i) ring opening and (ii) polymerization (Figure S14). These two side reactions were provoked with the model compound 4-Propylguaicol. The corresponding ^{1}H-^{13}C HSQC Spectra of these side reaction products is displayed in Figure S15 (A,B). As is shown in the spectra and in table S4, these side reaction products have distinct chemical shifts, allowing their detection by quick ^{1}H-^{13}C HSQC measurements.

In this case, the goal of the optimization of the reaction was chosen to obtain the highest possible selectivity towards the oxirane ring and to minimize the two main side reactions. Note that for some epoxy prepolymers the optimization goal is chosen in such a way as to obtain a reasonably high selectivity towards polymerization products (*i.e.* synthesis of novolacs).

The optimization of the reaction procedure was performed using the non-fractionated lignin oil. Since the solubility of the lignin oil in epichlorohydrin is excellent, it was not necessary to add a co-solvent (which is common in lignin glycidylation reactions). The temperature and reaction time of the first and second step were varied as well as the amount of NaOH added to the reaction medium. In Table S5 it is shown that the most selective conversion to the desired oxirane functionality is achieved in the reaction in which the first step of the process was carried out at a temperature of 85 ° C and the second step at room temperature.

This optimized reaction procedure was used to glycidylated the obtained lignin oligomers (P_1) and its derived fractions (F_1 to F_4). In Figure S16 the ^{1}H-^{13}C HSQC spectra of the glycidylated lignin fractions are shown. In a next step, the ^{1}H-^{13}C HSQC spectra of these glycidylated lignin fractions are overlayed with the ^{1}H-^{13}C HSQC spectra of the two side reaction products (Figure S17). Here, it is clearly showed that only in the case of the Parent lignin fraction (P_1) a minor side reaction (ring opening) occurs, as there are no other overlapping diagnostic peaks with the other fractions. This corresponds to the observation made in the reaction optimization step.

Based on the chemical shifts of these model compound reactions, we integrated these areas in the ^{1}H-^{13}C HSQC Spectra of the glycidylated lignin fractions to detect any undesired side reaction products. No polymerization reaction products were observed and only a minor number of ring opening products was found in the parent oligomeric fraction P1.

This led us to conclude that the incorporation of oxirane moieties in our RCF lignin fraction was highly selective, using this standard glycidylation protocol.

b. Aliphatic hydroxyl reactivity

Besides the two main possible side reactions, the reactivity of the 4-propanol side chain was also studied by reacting the model compound 3-phenyl-1-propanol in glycidylation procedure. We found that oxirane moieties could be introduced on these aliphatic alcohols (Figure S15, D). Based on these chemical shifts, we integrated the diagnostic area in the ^{1}H-^{13}C HSQC spectra of the glycidylated lignin fractions and found little incorporation of oxirane moieties on the aliphatic side chain (Table S6). This is also confirmed by a decrease of the 4-propanol/4-propyl ratio before and after glycidylation, assuming that the 4-propyl chain is unreactive (Table S7). Likely, this explains why the experimental EEW is slightly lower than the calculated EEW, the latter being solely dependent on the phenolic OH content of the lignin fractions.

E. Supplementary note 5

It is clearly shown that the width of the DTGA curves is broader for the RCF lignin-based epoxy resins compared to the BADGE epoxy resin (Figure S29), indicating less homogeneous samples (which is supported by the dispersity Index).

The DTGA curves further demonstrate that the epoxy resin based on F_4 start losing mass more rapidly compared to the resins based on P_1 and F_1-F_3. These four samples start losing their mass at more or less the same temperature, as is reflected by the similar $T_{d,5\%}$. On the other hand, the BADGE-based epoxy resins start losing mass at a higher temperature. Similar observations were made in previous papers, wherein lignin-derived molecules were used as a precursor for synthesizing lignin-based epoxy resins and were benchmarked again BADGE-based epoxy resins.[4]

The epoxy resins based on the highest molecular weight RCF lignin fractions (F_1) loses mass less rapidly than the 2nd highest molecular weight RCF lignin fractions (F_2), which in turn loses mass less rapidly than F_3, F_4 and P_1 as is shown by the derivative of their TGA thermogram at a temperature between 300-360 °C.

On the other hand, the epoxy resins based on F_1 loses more mass than in respective order F_2, F_3-P_1, F_4 at a temperature between 360 – 500 °C.

A possible explanation for this observation is that the higher molecular weight RCF lignin fractions have a higher degree of cross-linking, resulting in more bonds to break to release a molecule.[4]

3. Supplementary Figures

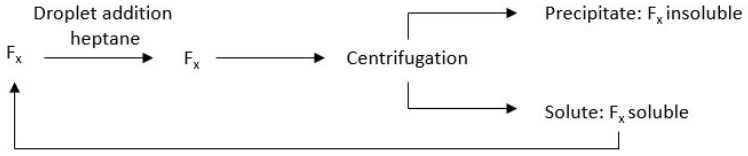

Figure S1. Schematic representation of the fractionation based on solvent-anti-solvent precipitation.

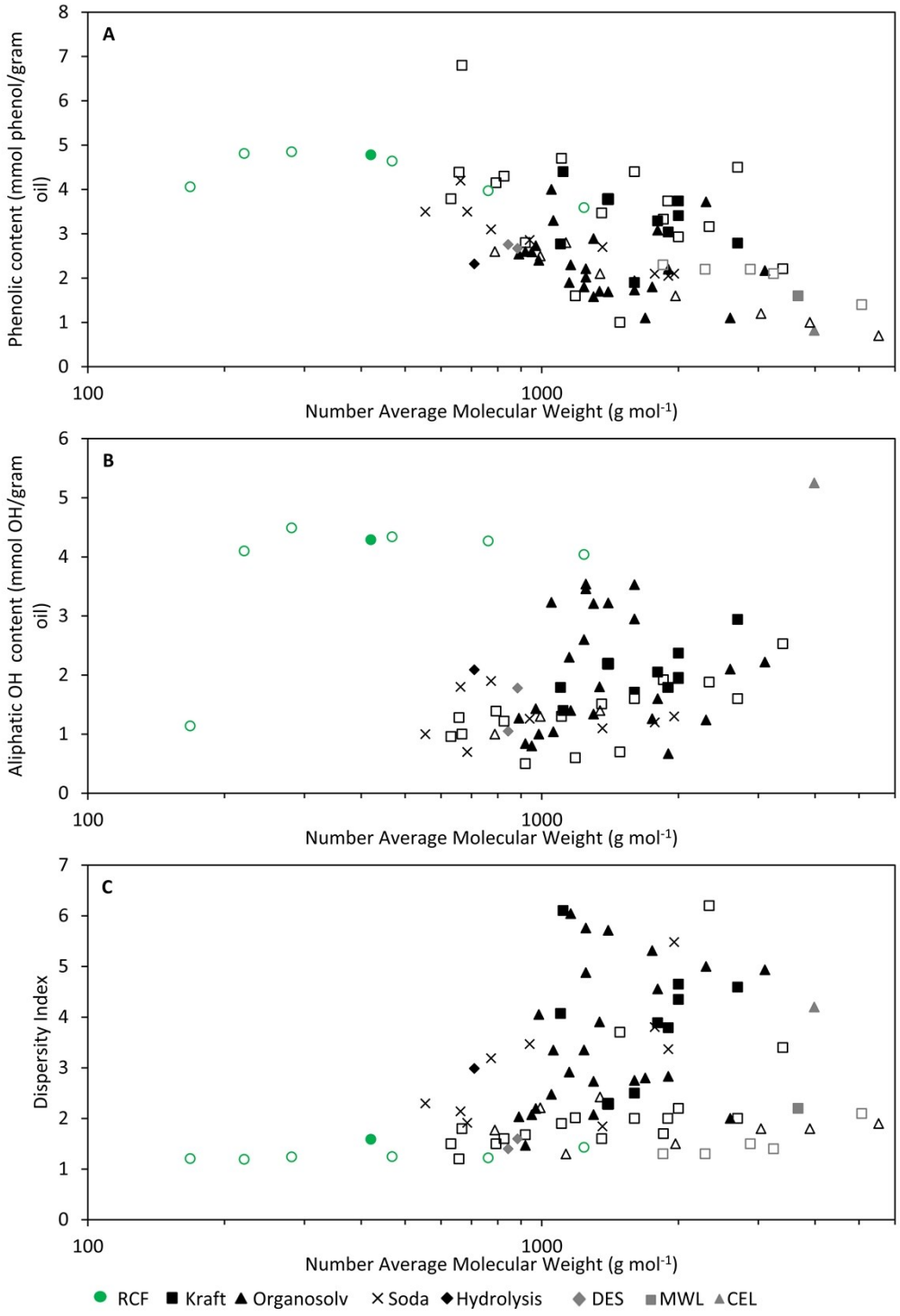

Figure S2. A. Overview of the total phenolic content to the M_n of a variety lignins reported in literature. **B.** Overview of the total aliphatic content to the M_n of a variety of lignins reported in literature. **C.** Overview of the dispersity index to the M_n of a variety of lignins reported in literature. The values are based on Table S1. A filled symbol indicates an unfractionated lignin, empty symbols indicate that it is a lignin fraction.

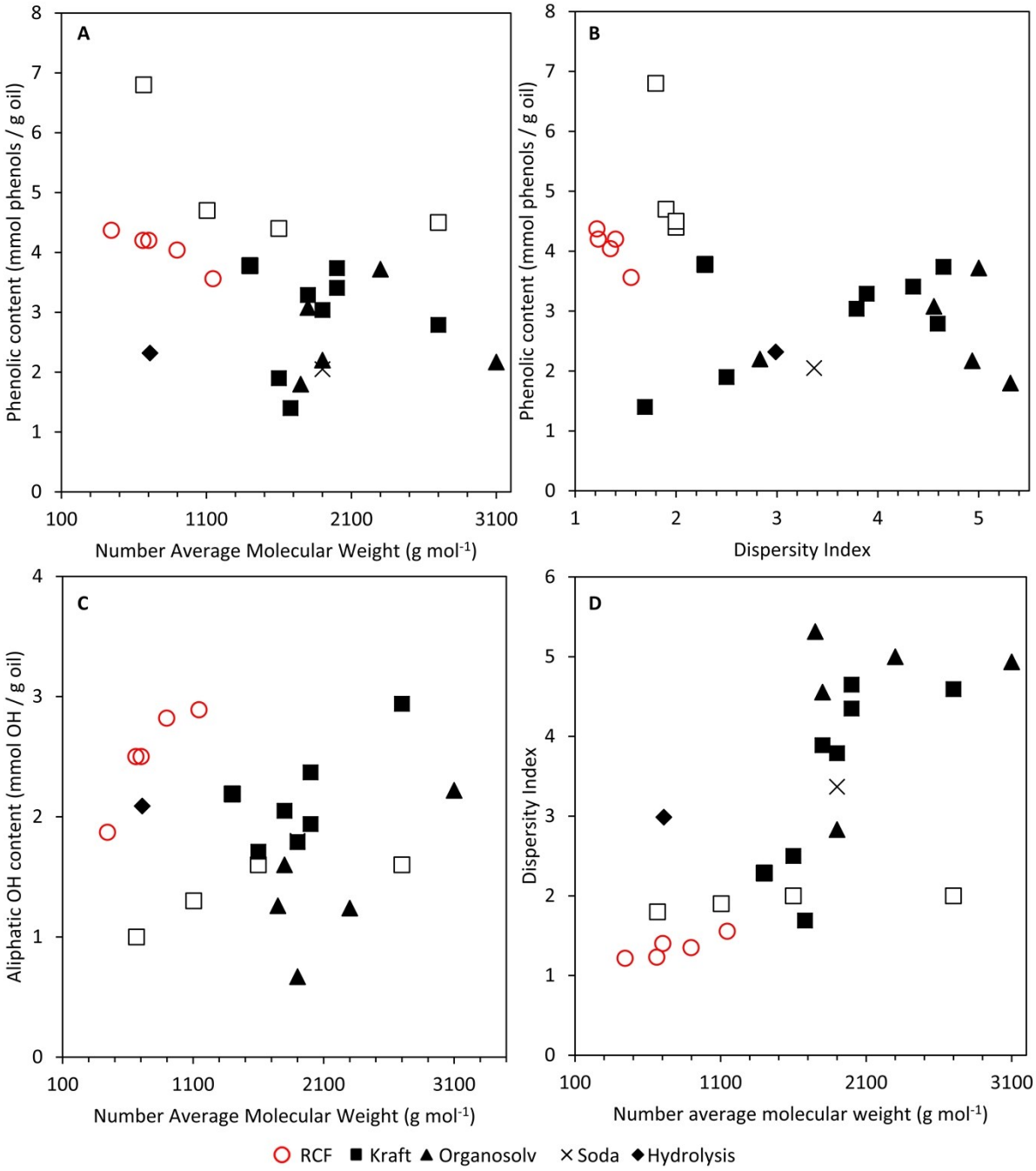

Figure S3. A. Overview of the total phenolic content to the M_n of lignins reported in literature used in lignin-epoxy resin synthesis. **B.** Overview of the total phenolic content to the dispersity index of lignins reported in literature used in lignin-epoxy resin synthesis. **C.** Overview of the aliphatic hydroxyl content to the M_n of lignins reported in literature used in lignin-epoxy resin synthesis. **D.** Overview of the dispersity index to the M_n of lignins reported in literature used in lignin-epoxy resin synthesis. The values are based on Table S8. A filled symbol indicates an unfractionated lignin, empty symbols indicate that it is a lignin fraction.

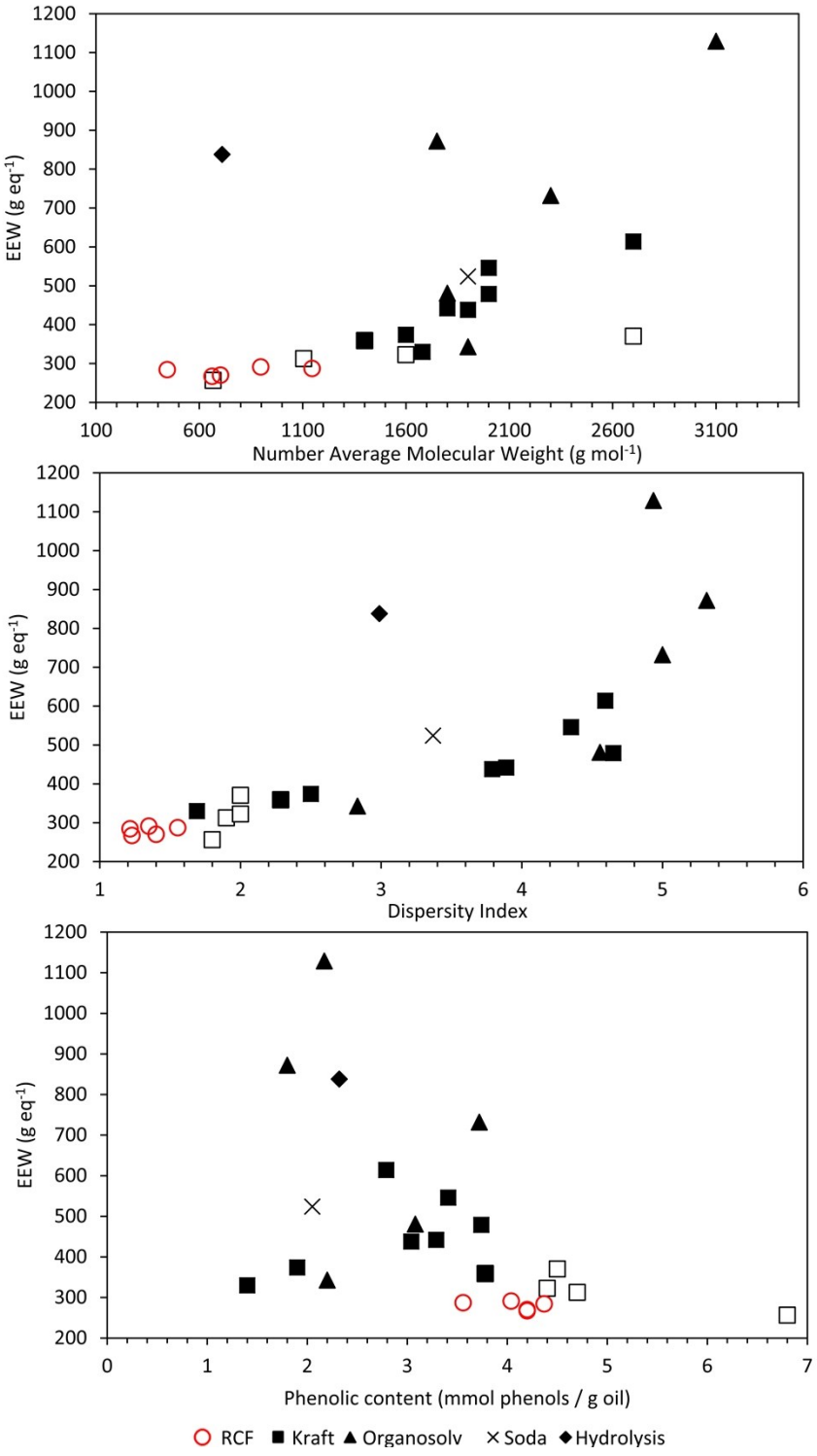

Figure S4. A. Overview of the EEW to the M_n of lignins reported in literature used in lignin-epoxy resin synthesis. **B.** Overview of EEW to the dispersity index of lignins reported in literature used in lignin-epoxy resin synthesis. **C.** Overview of the EEW to the initial phenolic content of lignins reported in literature used in lignin-epoxy resin synthesis. The values are based on Table S8. A filled symbol indicates an unfractionated lignin, empty symbols indicate that it is a lignin fraction.

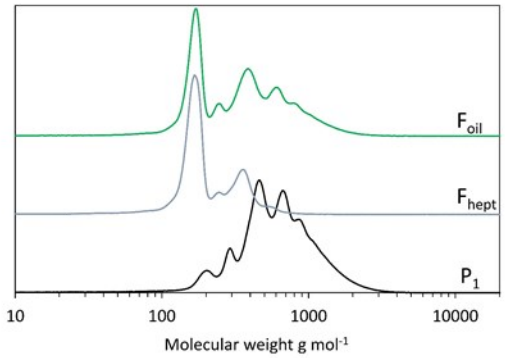

Figure S5. GPC profile of the lignin oil after RCF (F_{oil}) and its heptane soluble extract (F_{hept}) and insoluble residu (P_1)

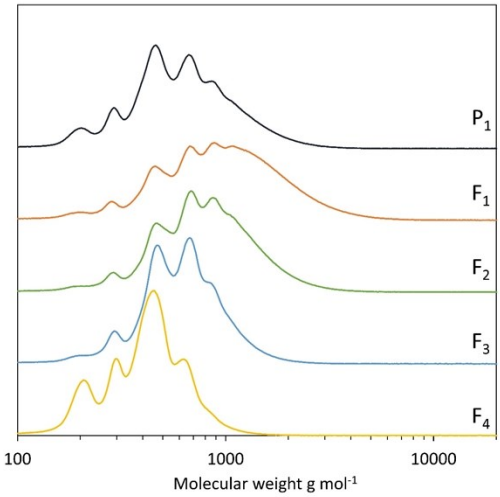

Figure S6. GPC profile of the RCF oligomers P_1 and its fractionated streams F_1 to F_4.

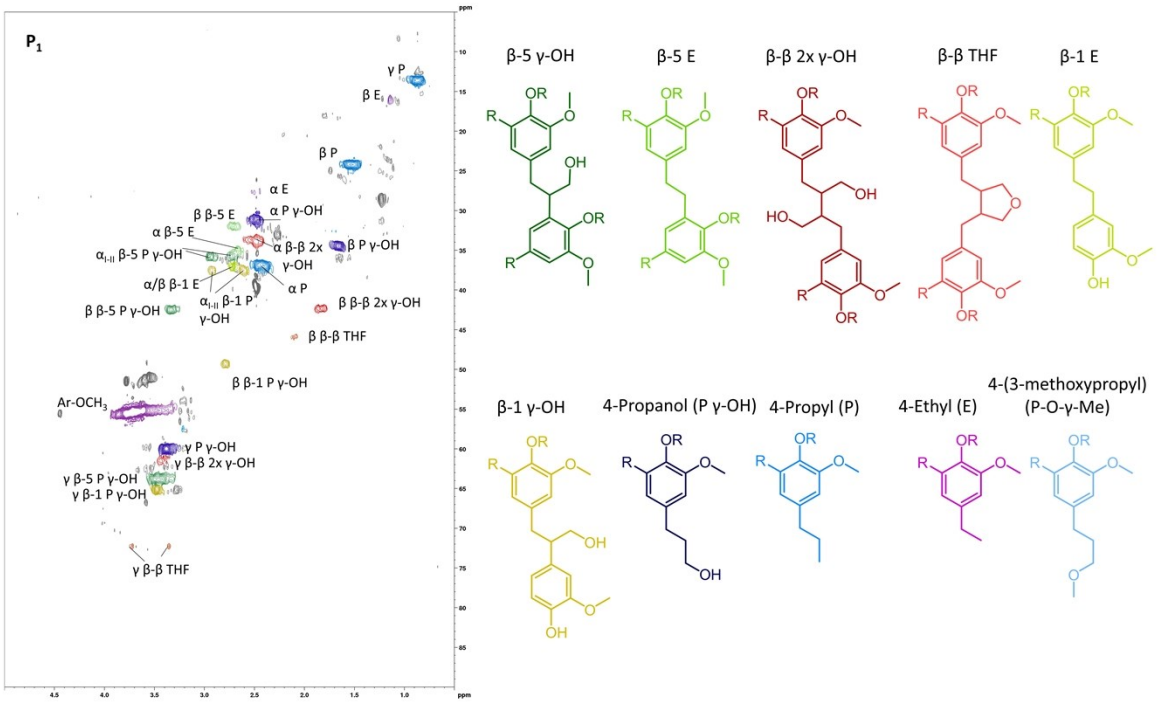

Figure S7. Assignment of the molecular RCF lignin structures present in P_1 by ^{1}H-^{13}C HSQC spectroscopy.

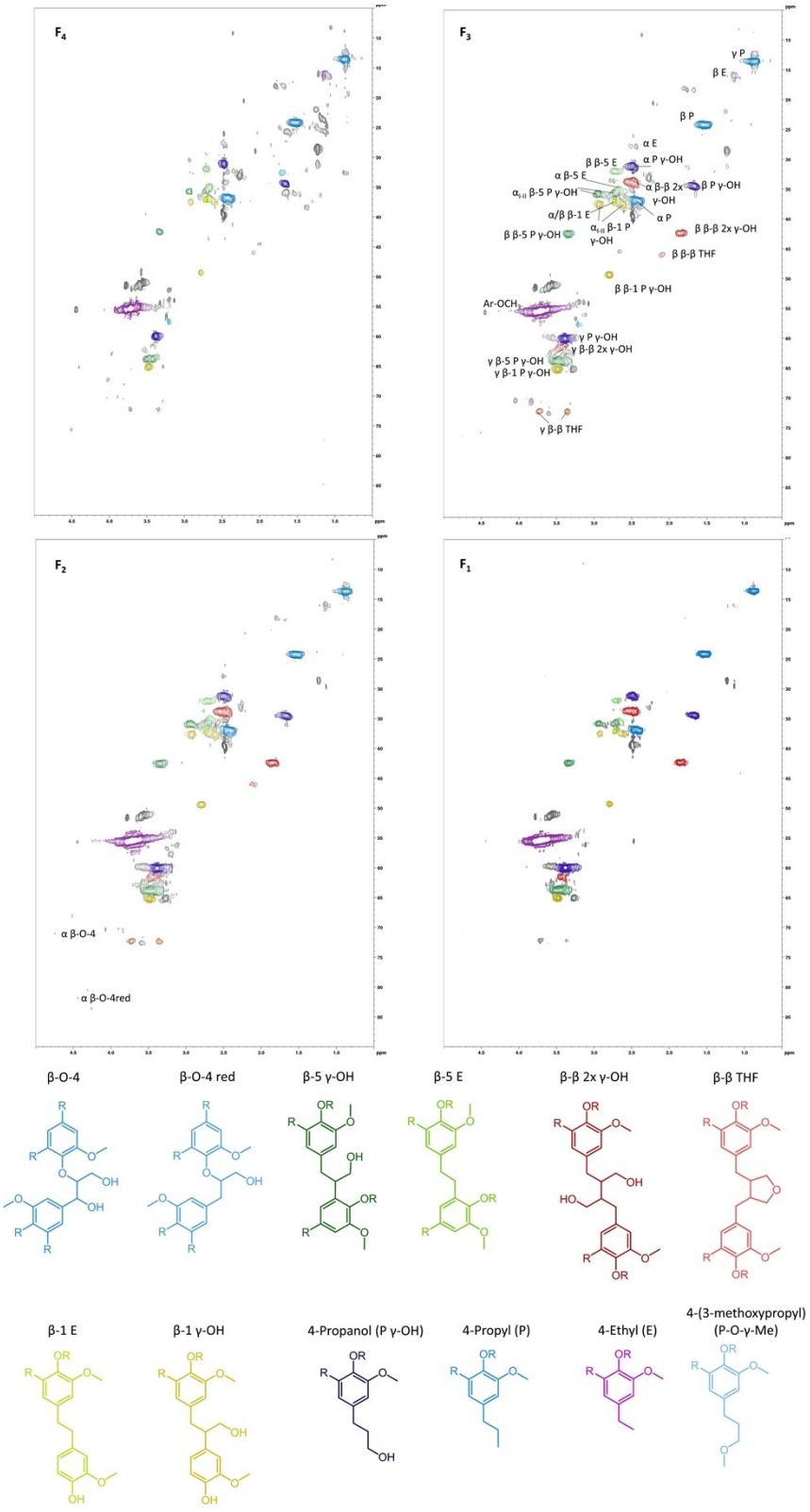

Figure S8 ^{1}H-^{13}C HSQC spectra of the F_1-F_4 fractions.

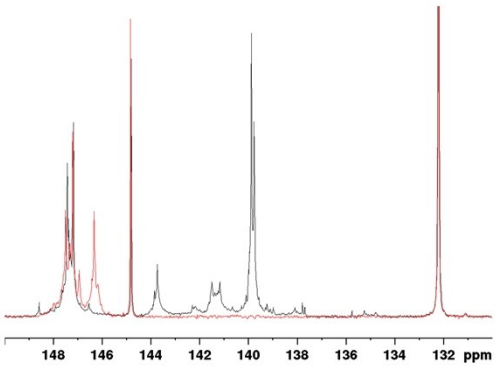

Figure S9. ^{31}P-NMR spectrum of P_1 before glycidylation (black) and after glycidylation (red).

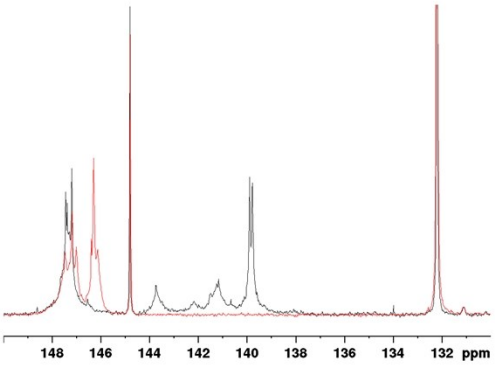

Figure S10. ^{31}P-NMR spectrum of F_1 before glycidylation (black) and after glycidylation (red).

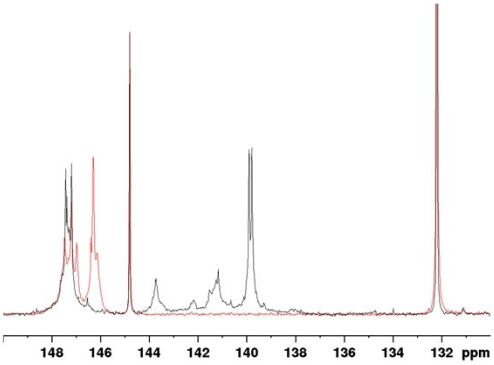

Figure S11. ^{31}P-NMR spectrum of F_2 before glycidylation (black) and after glycidylation (red).

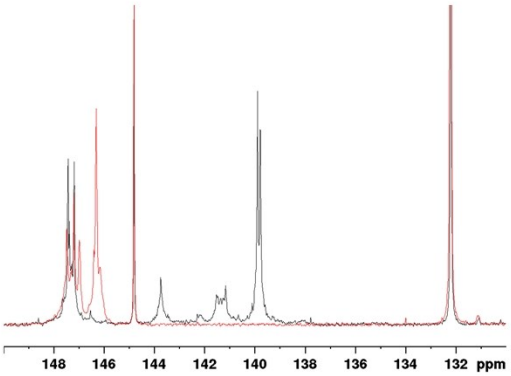

Figure S12. ^{31}P-NMR spectrum of F_3 before glycidylation (black) and after glycidylation (red).

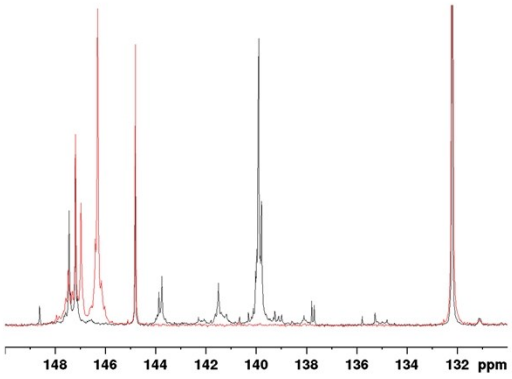

Figure S13. ^{31}P-NMR spectrum of F_4 before glycidylation (black) and after glycidylation (red).

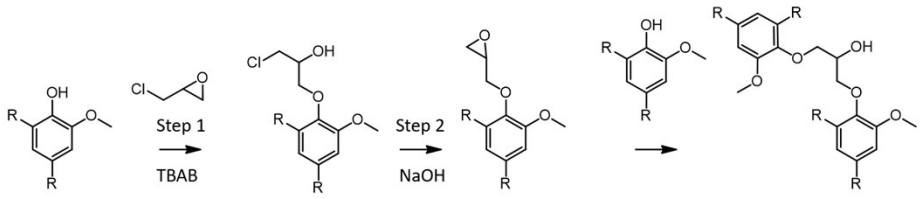

Figure S14. Two step glycidylation procedure to introduce oxirane moieties on RCF lignin as well as the possible side reaction products.

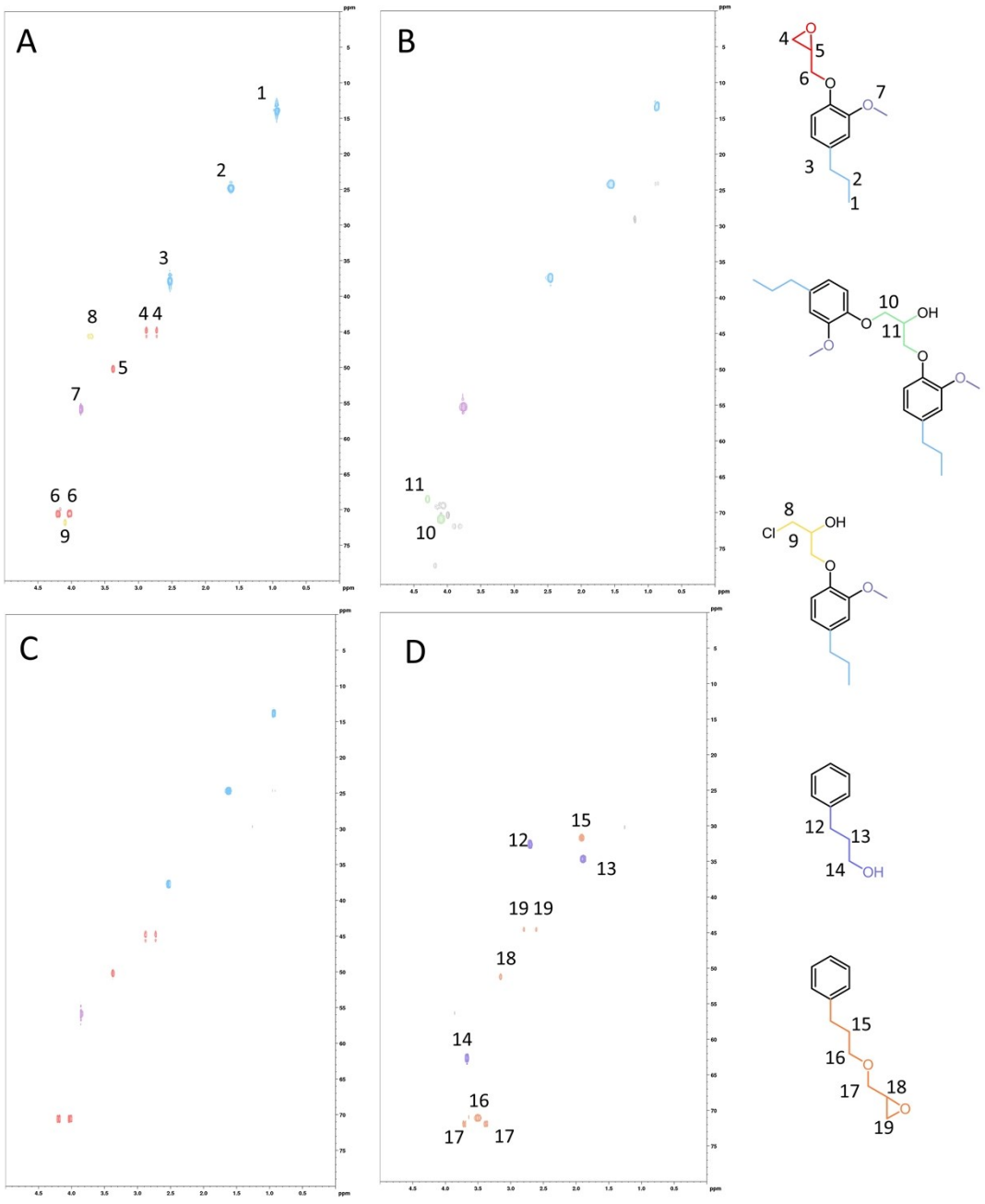

Figure S15. Signals of the possible (side)-reaction products in the ^{1}H-^{13}C HSQC Spectroscopy spectrum. A: reaction of 4-Propylguaiacol according to the glycidylation reaction conditions without addition of NaOH in the second step, impeding the ring closure. B: Reaction of 4-Propylguaiacol according to the glycidylation reaction conditions with 0.5 eq. Epichlorohydrin, promoting the dimerization. C: Reaction of 4-Propylguaiacol according to the glycidylation reaction conditions. D:Reaction of 3-phenyl-1-propanol according to the glycidylation reaction conditions, showing that the aliphatic OH can be partly glycidylated.

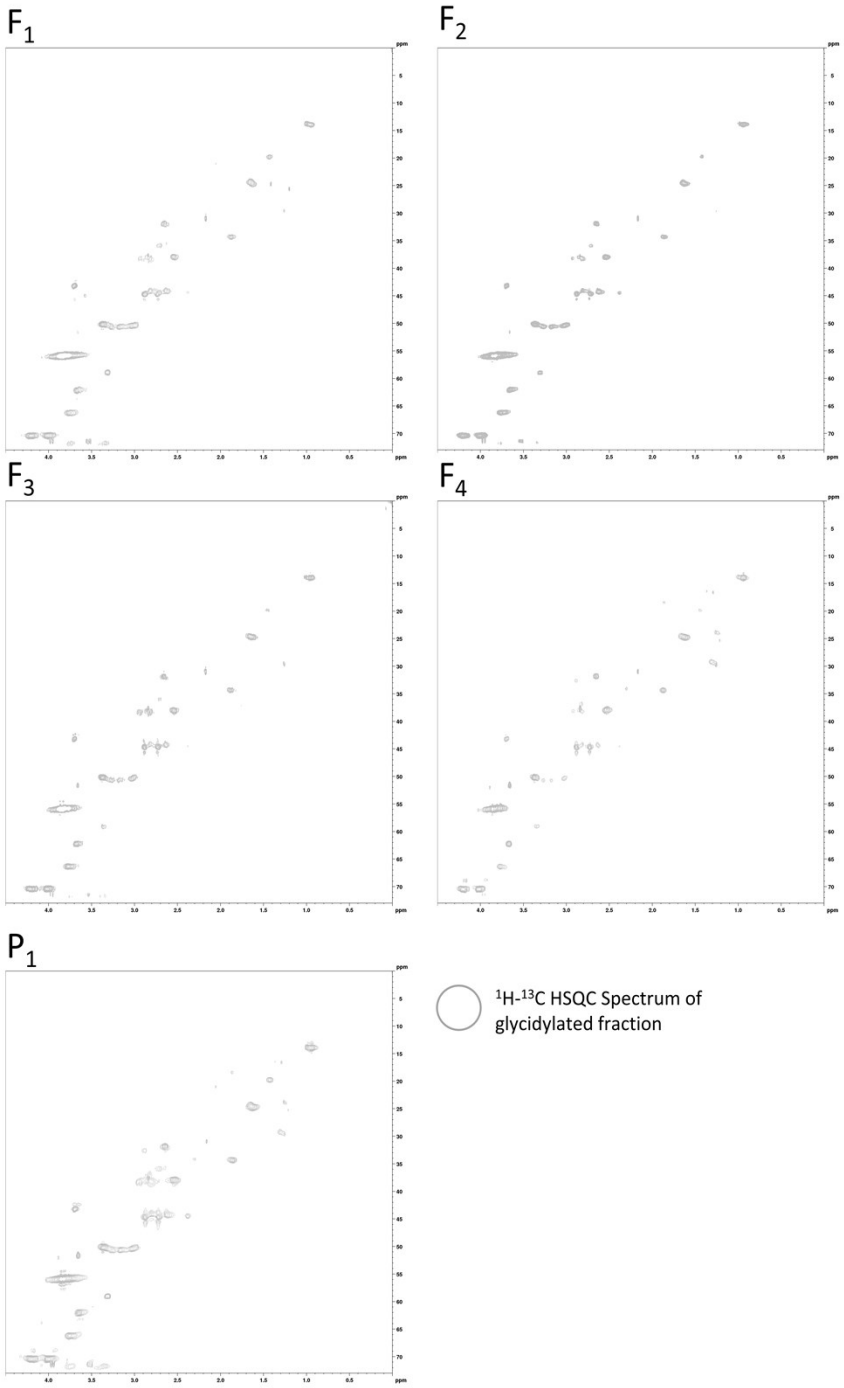

Figure S16. ^{1}H-^{13}C HSQC spectra of the glycidylated lignin P_1 and F_1-F_4.

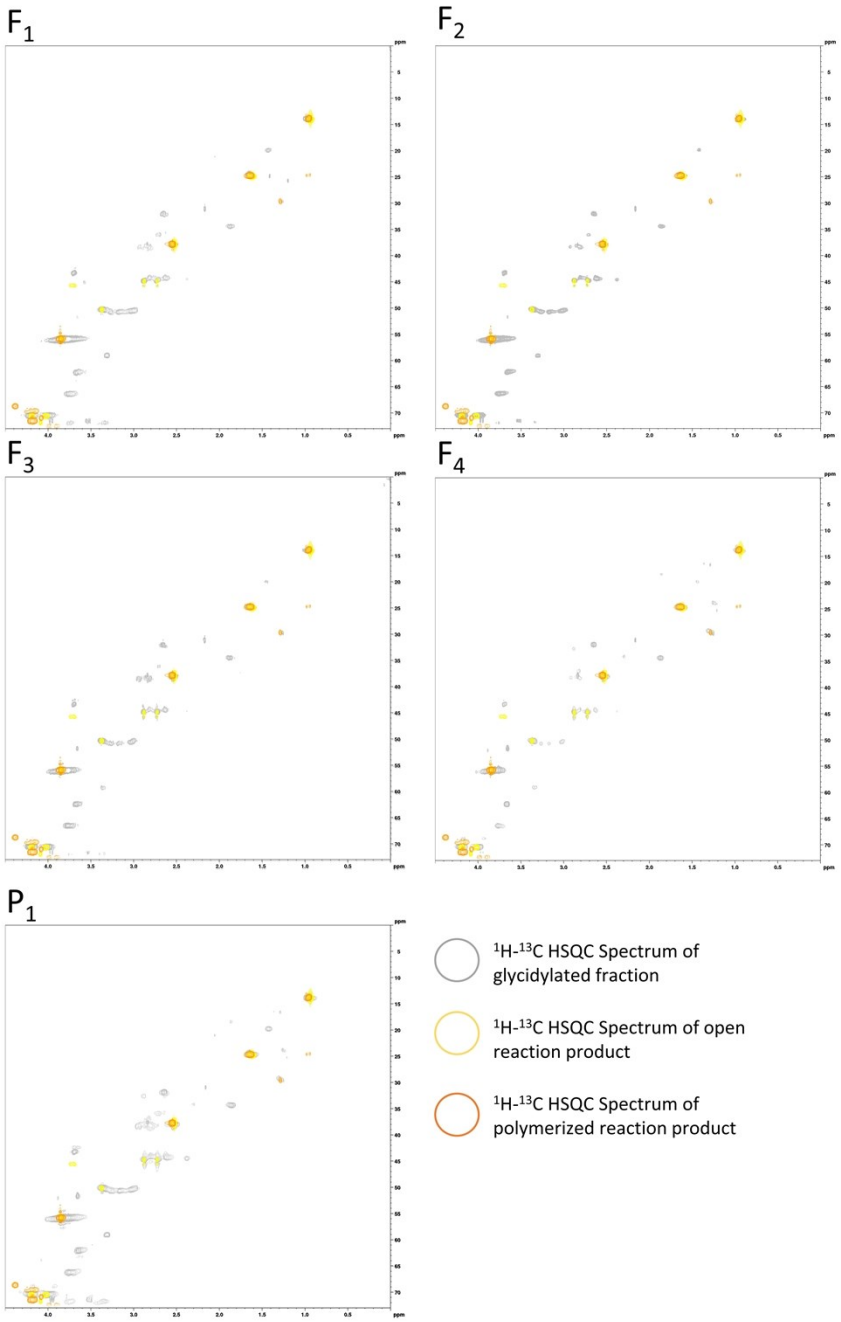

Figure S17. ^{1}H-^{13}C HSQC spectra of the glycidylated lignin P_1 and F_1-F_4, overlayed with the $_{1}H$-$_{13}C$ HSQC spectra of the two main side-reaction products: (i) the spectrum of an open reaction product, (ii) the spectrum of a polymerization reaction product.

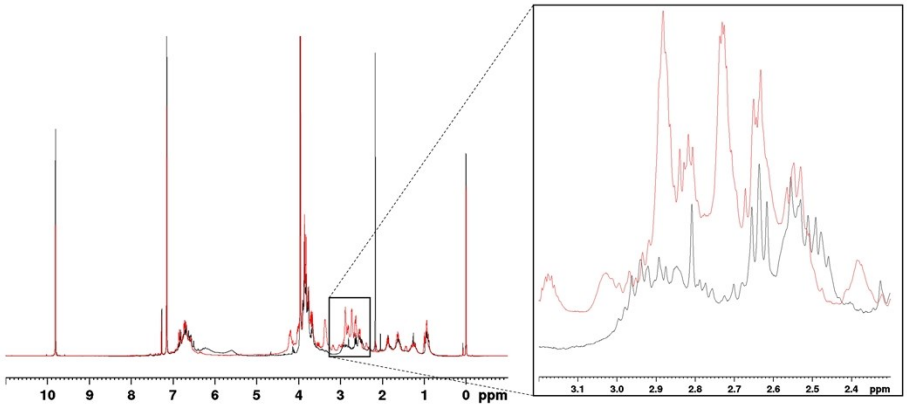

Figure S18. ^{1}H-NMR spectrum of P_1 before glycidylation (black) and after glycidylation (red).

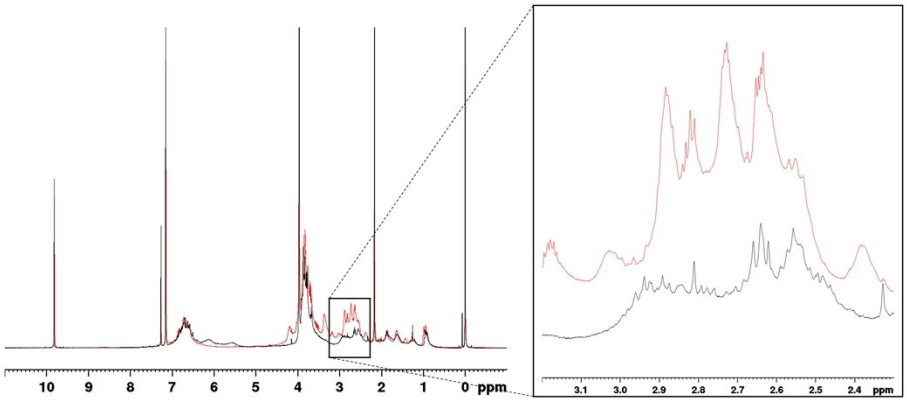

Figure S19. ^{1}H-NMR spectrum of F_1 before glycidylation (black) and after glycidylation (red).

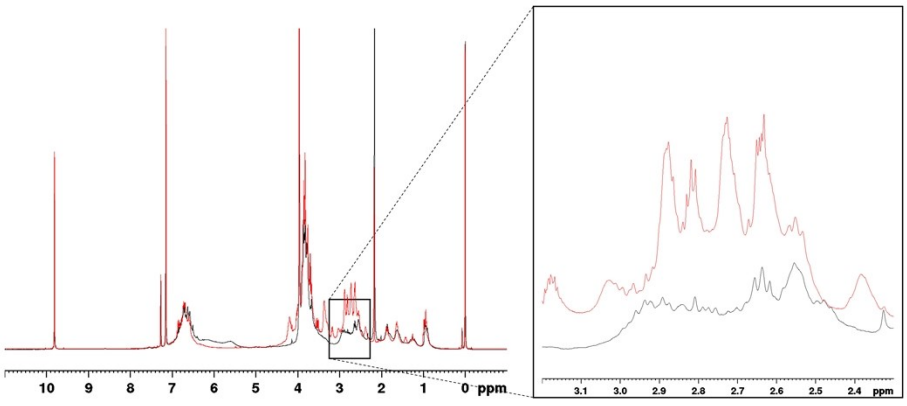

Figure S20. ^{1}H-NMR spectrum of F_2 before glycidylation (black) and after glycidylation (red).

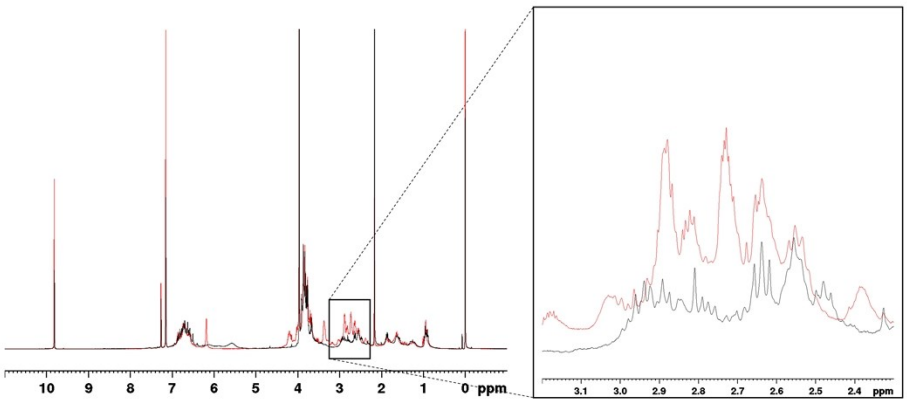

Figure S21. ^{1}H-NMR spectrum of F_3 before glycidylation (black) and after glycidylation (red).

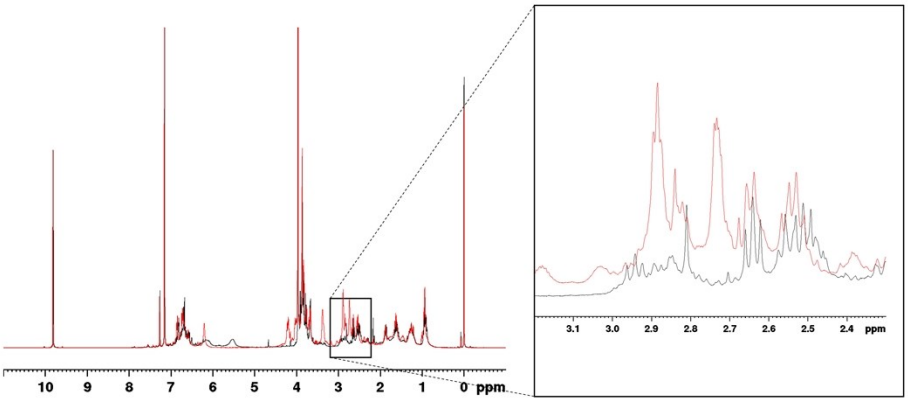

Figure S22. ^{1}H-NMR spectrum of F_4 before glycidylation (black) and after glycidylation (red).

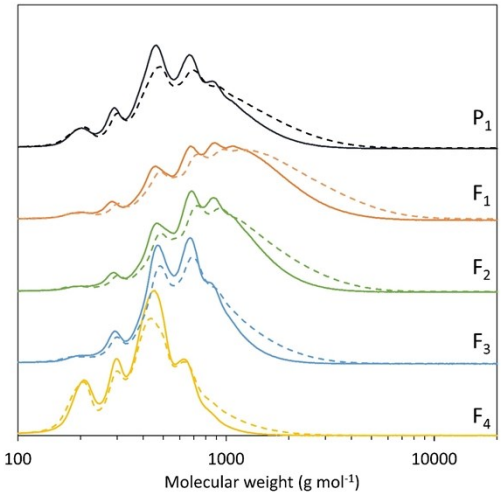

Figure S23. GPC profile of the lignin fractions before glycidylation (solid lines) and after glycidylation (dashed lines) relative to the molecular weight.

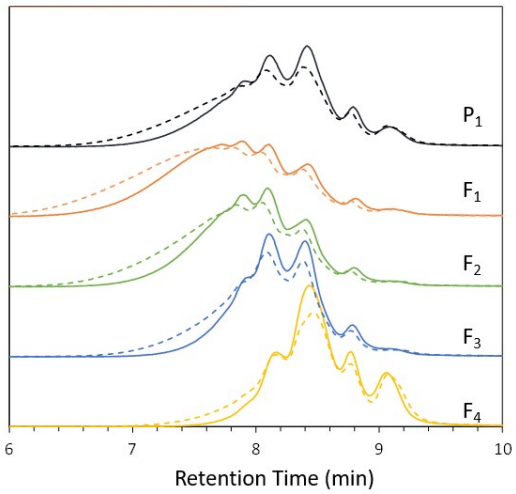

Figure S24. GPC profile of the lignin fractions before glycidylation (solid lines) and after glycidylation (dashed lines).

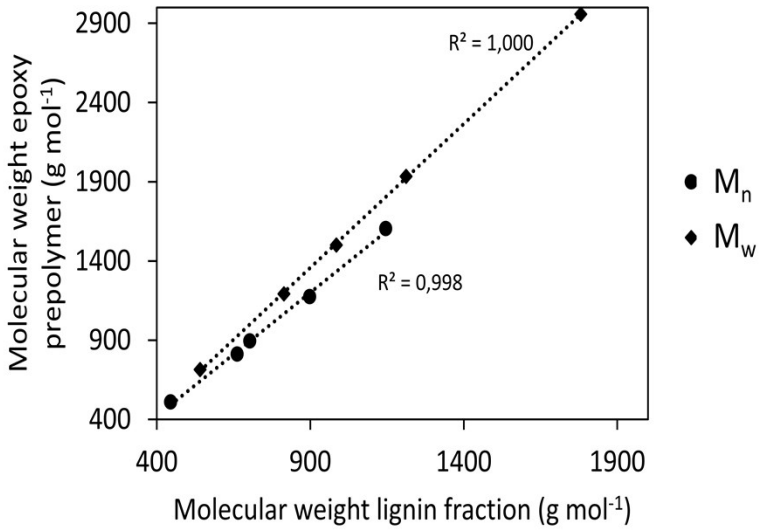

Figure S25. Correlation between M_n and M_w of P_1 and F_1-F_4 before and after glycidylation.

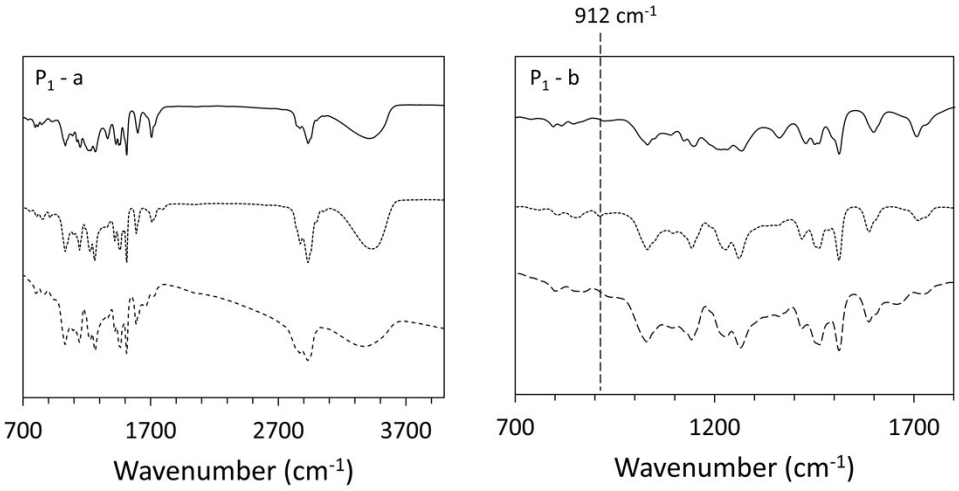

Figure S26. FT-IR spectrum of the P_1 lignin fraction (full line), the glycidylated P_1 lignin fraction (dotted line) and the DETA-cured P_1 lignin fraction (dashed line). Spectrum a is the full FT-IR spectrum, spectrum b is the spectrum between 700-1800 cm^{-1}.

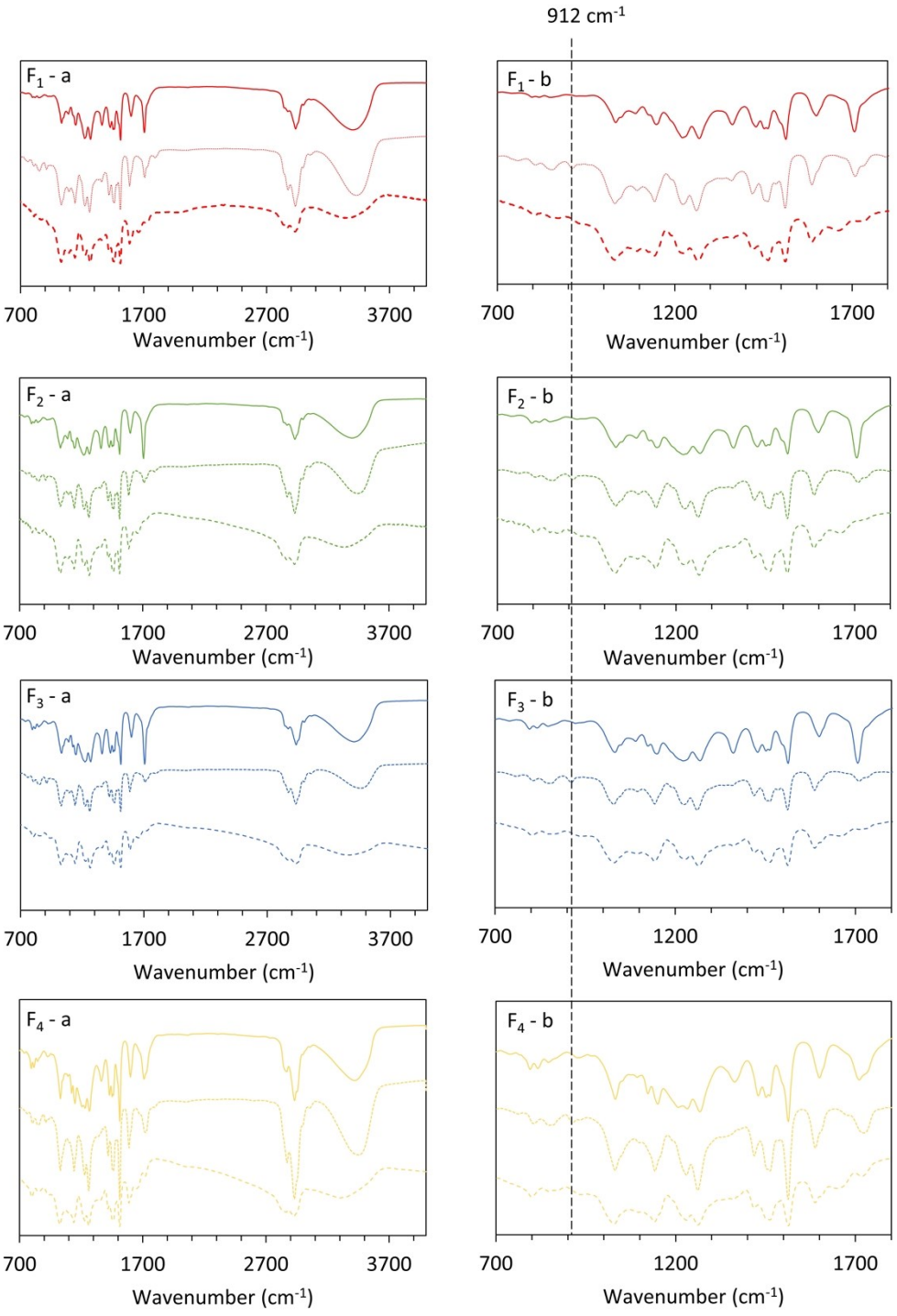

Figure S27. FT-IR spectra of the F_1-F_4 lignin fractions (full line), the glycidylated F_1-F_4 lignin fractions (dotted line) and the DETA-cured F_1-F_4 lignin fractions (dashed line). Spectrum a is the full FT-IR spectrum, spectrum b is the spectrum between 700-1800 cm^{-1}.

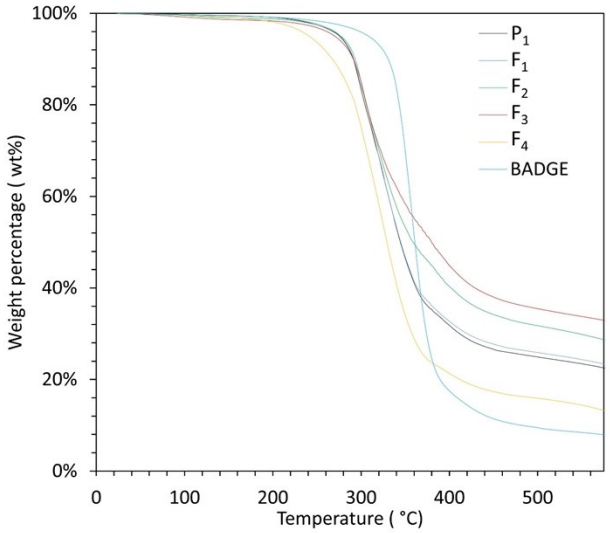

Figure S28. TGA thermograms of the cured epoxy networks as function of temperature. The temperature ranged between 20 and 575 °C under N_2 flow (ramp of 10 °C min^{-1}).

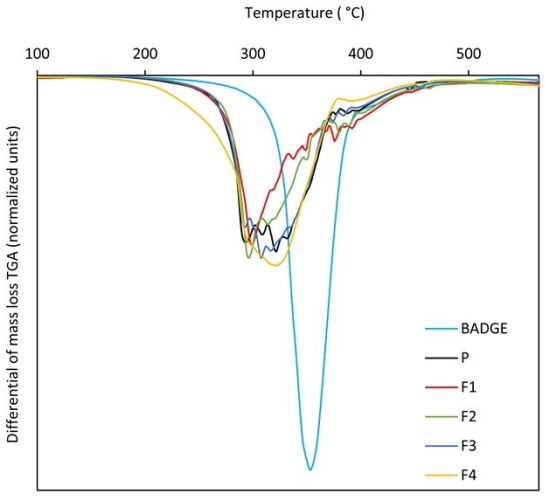

Figure S29. DTGA curve of the cured epoxy networks as function of temperature.

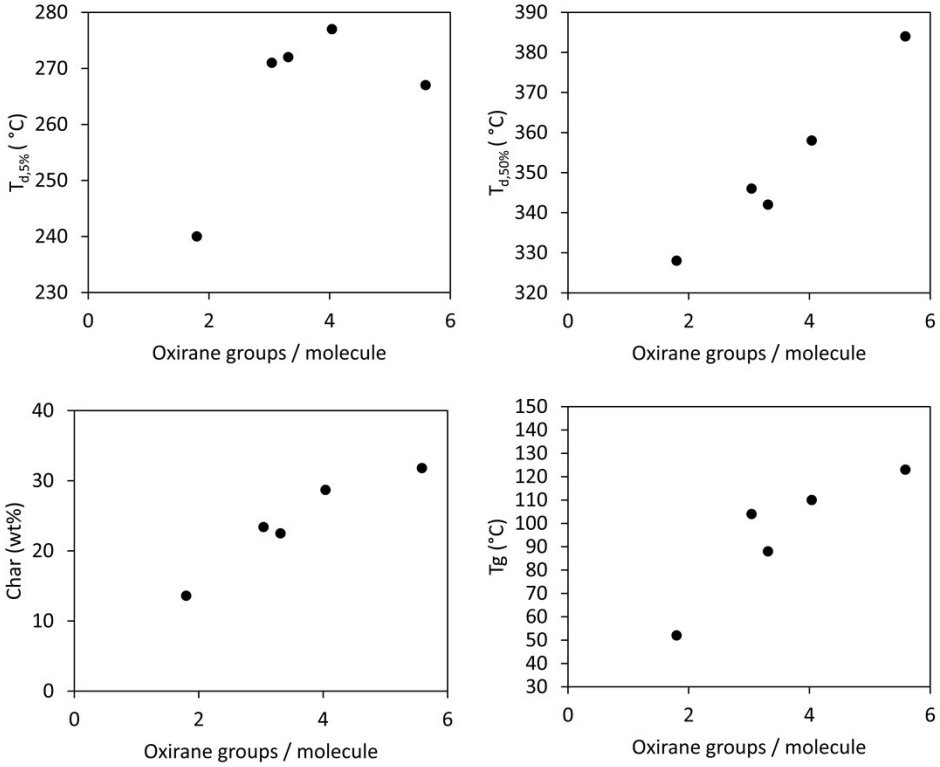

Figure S30. Thermal properties of the cured epoxy resins relative to the average number of oxirane moieties per molecule in the respective fractions.

4. Supplementary tables

Table S1. Overview of the molecular weights and hydroxyl functionalities of a variety of lignins and lignin-derived fractions in literature.

Entry	Ref	Lignin Type	Mn (g/mol)	Mw (g/mol)	Phenolic OH (mmol / g)	Aliphatic OH (mmol / g)	Type	Fraction
1	[5]	Kraft - Softwood (1)	1800	7000	3,29	2,05	Kraft	No
2	"	Kraft - Hardwood (1)	2700	12400	2,79	2,94	Kraft	No
3	"	Soda - Hardwood	1900	6400	2,05	1,8	Soda	No
4	"	Organosolv - Corn Stover	1900	5380	2,2	0,67	Organosolv	No
5	"	Organosolv - Bagasse	2300	11500	3,72	1,24	Organosolv	No
6	"	Organosolv - Peanut Shell	1750	9300	1,8	1,26	Organosolv	No
7	"	Organosolv - Hardwood	1800	8200	3,08	1,6	Organosolv	No
8	"	Kraft - Softwood (2)	2000	8700	3,41	1,94	Kraft	No
9	"	Kraft - Softwood (3)	1900	7200	3,04	1,79	Kraft	No
10	"	Kraft - Hardwood (2)	1600	4000	1,9	1,71	Kraft	No
11	"	Kraft - Hardwood (3)	1400	3200	3,78	2,19	Kraft	No
12	"	Organosolv - Wheat Straw	3100	15300	2,17	2,22	Organosolv	No
13	"	Kraft - Softwood (4)	2000	9300	3,74	2,37	Kraft	No
14	[6]	Kraft - Softwood - Parent	1114	6800	4,4	1,4	Kraft	No
15	"	Kraft - Softwood - LF EtoAc	667	1200	6,8	1	Kraft	Yes
16	"	Kraft-Softwood - LF EtOH	1105	2100	4,7	1,3	Kraft	Yes
17	"	Kraft - Softwood - LF MeOH	1600	3200	4,4	1,6	Kraft	Yes
18	"	Kraft - Softwood - LF Acetone	2700	5400	4,5	1,6	Kraft	Yes
19	[7]	Indulin Kraft	1176	5056,8			Kraft	No
20	"	Indulin Kraft - Etoac	631	946,5	3,79	0,96	Kraft	Yes
21	"	Indulin Kraft - 5% MeOH/Etoac	657	788,4	4,39	1,28	Kraft	Yes
22	"	Indulin Kraft - 10% MeOH/EtoAc	793	1189,5	4,15	1,39	Kraft	Yes
23	"	Indulin Kraft - 20% MeOH / EtoAc	1355	2168	3,47	1,51	Kraft	Yes

Entry		Lignin Type	Mn (g/mol)	Mw (g/mol)	Phenolic OH (mmol / g)	Aliphatic OH (mmol / g)	Type	Fraction
24	"	Indulin Kraft - 30% MeOH / EtoAc	1853	3150,1	3,33	1,92	Kraft	Yes
25	"	Indulin Kraft - MeOH	2000	4400	2,93	1,96	Kraft	Yes
26	"	Indulin Kraft - MeOH insoluble	3396	11546,4	2,21	2,53	Kraft	Yes
27	[8]	P1000 F1	685	1312	3,5	0,7	Soda	Yes
28	"	P1000 F2	1360	2508	2,7	1,1	Soda	Yes
29	"	P1000 F3	1773	6747	2,1	1,2	Soda	Yes
30	"	P1000 F4	1957	10728	2,1	1,3	Soda	Yes
31	"	High Temp Ethanol/Water Wheat Straw F1	788	1396	2,6	1	Organosolv	Yes
32	"	High Temp Ethanol/Water Wheat Straw F2	992	2194	2,5	1,3	Organosolv	Yes
33	"	High Temp Ethanol/Water Wheat Straw F3	1343	3253	2,1	1,4	Organosolv	Yes
34	"	RAIZ Eucalyptus EtOAc	920	1543	2,8	0,5	Kraft	Yes
35	"	RAIZ Eucalyptus 10% EtOAc/MeOH	1185	2386	1,6	0,6	Kraft	Yes
36	"	RAIZ Eucalyptus MeOH	1486	5503	1	0,7	Kraft	Yes
37	"	Alcell	985	3991	2,4	1	Organosolv	No
38	"	Sigma-Aldrich organosolv	1158	6999	2,3	1,4	Organosolv	No
39	"	ECN Low Temp Ethanol/Water Wheat Straw	1149	3350	1,9	2,3	Organosolv	No
40	"	ECN Low Temp Ethanol/Water Pine	1239	4152	1,8	2,6	Organosolv	No
41	"	ECN Low Temp Acetone/Water Wheat Straw	1340	5232	1,7	1,8	Organosolv	No
42	[9]	CEL - Poplar	3984,048	16733	0,82	5,25	CEL	No
43	"	ChCl-Pb-3h lignin	884	1414	2,67	1,78	DES	No

Entry	Authors	Lignin Type	Mn (g/mol)	Mw (g/mol)	Phenolic OH (mmol / g)	Aliphatic OH (mmol / g)	Type	Fraction
44	[9]	ChCl-PB- 9h lignin	843	1180	2,76	1,05	DES	No
45	[10]	Kraft - AMKL-15K	2337	14488	3,16	1,88	Kraft	Yes
46	"	Kraft - AMKL 4-K	1895	3790	3,74	1,79	Kraft	Yes
47	"	Kraft - AMKL - 1k	826	1322	4,3	1,22	Kraft	Yes
48	[11]	Indulin - Kraft - Softwood	1100	4480	2,77	1,79	Kraft	No
49	"	Soda P1000 - Wheat Straw + Grass	940	3260	2,86	1,26	Soda	No
50	"	Alcell: Organosolv - Mixed Hardwood	1060	3550	3,3	1,04	Organosolv	No
51	"	Organosolv - Wheat Straw	890	1810	2,54	1,27	Organosolv	No
52	"	Organosolv - Poplar	950	1970	2,59	0,8	Organosolv	No
53	"	Organosolv - Spruce	970	2130	2,73	1,43	Organosolv	No
54	[12]	Protobind lignin	773	2465	3,1	1,9	Soda	No
55	"	Protobind lignin soluble in methanol	662	1417	4,2	1,8	Soda	Yes
56	"	Protobind lignin soluble in ethanol	554	1273	3,5	1	Soda	Yes
57	[13]	Organosolv (ethanol/water) - Birch (1)	1250	7200	2,02	3,46	Organosolv	No
58	"	Organosolv (ethanol/water) - Birch (2)	1400	8000	1,69	3,22	Organosolv	No
59	"	Organosolv (ethanol/water) - Birch (3)	1300	3550	1,58	3,21	Organosolv	No
60	"	Organosolv (ethanol/water) - Birch (4)	1600	4400	1,73	3,53	Organosolv	No
61	"	Organosolv (ethanol/water) - Birch (5)	1250	6100	2,21	3,54	Organosolv	No
62	"	Organosolv (ethanol/water) - Birch (6)	1300	2700	2,89	1,34	Organosolv	No
63	"	Organosolv (ethanol/water) - Birch (7)	1600	4400	1,94	2,95	Organosolv	No
64	[14]	MWL - Poplar	3670	8070	1,6		MWL	No
65	"	MWL Poplar F1	1850	2410	2,3		MWL	Yes
66	"	MWL Poplar F2	2290	2980	2,2		MWL	Yes
67	"	MWL Poplar F3	2880	4320	2,2		MWL	Yes

Entry	Authors	Lignin Type	Mn (g/mol)	Mw (g/mol)	Phenolic OH (mmol / g)	Aliphatic OH (mmol / g)	Type	Fraction
68	[14]	MWL Poplar F4	3240	4540	2,1		MWL	Yes
69	"	MWL Poplar F5	5070	10640	1,4		MWL	Yes
70	"	Organosolv (ethanol/water) - Poplar	1690	4730	1,1		Organosolv	No
71	"	Organosolv (ethanol/water) - Poplar F1	1130	1470	2,8		Organosolv	Yes
72	"	Organosolv (ethanol/water) - Poplar F2	1970	2960	1,6		Organosolv	Yes
73	"	Organosolv (ethanol/water) - Poplar F3	3040	5470	1,2		Organosolv	Yes
74	"	Organosolv (ethanol/water) - Poplar F4	3895	7010	1		Organosolv	Yes
75	"	Organosolv (ethanol/water) - Poplar F5	5520	10490	0,7		Organosolv	Yes
76	[15]	EtOH Organosolv - Poplar	920	1350	2,6	0,84	Organosolv	No
77	"	CELF Organosolv Poplar	1050	2600	4	3,23	Organosolv	No
78	"	GVL Organosolv Poplar	2600	5200	1,1	2,1	Organosolv	No
86	[16]	RCF - Pine - Foil	420	667	4,78	4,29	RCF	No
87	"	RCF - Pine - FH100	168	203	4,06	1,14	RCF	Yes
88	"	RCF - Pine - FH80	221	264	4,81	4,1	RCF	Yes
89	"	RCF - Pine - FH60	281	349	4,85	4,49	RCF	Yes
90	"	RCF - Pine - FH40	468	584	4,64	4,34	RCF	Yes
91	"	RCF - Pine - FH20	762	931	3,97	4,27	RCF	Yes
92	"	RCF - Pine - FEA100	1239	1771	3,59	4,04	RCF	Yes
93	[17]	Depolymerized Hydrolysis lignin	710	2121	2.32	2.09	Hydrolysis	No
94	[18]	Kraft - Softwood	1680	2840	1.4		Kraft	No

Table S2. Relative quantification of the molecular structures present in P_1 and F_1-F_4 by ^{1}H-^{13}C HSQC spectroscopy.

	β-O-4	β-O-4 red	β-β 2x γ-OH	β-β THF	β-1 γ-OH	β-1 E	β-5 γ-OH	β-5 E	5-5	4-P	4-POH	4-PO-Me	4-E	4-M
P_1	0.6%	1.2%	7.5%	2.9%	7.2%	2.8%	13.4%	4.2%	19.1%	23.5%	14.8%	0.5%	2.0%	0.4%
F_1	3.7%	1.0%	16.1%	2.1%	6.1%	1.5%	13.9%	4.2%	21.2%	15.7%	13.5%	0.4%	0.6%	0.0%
F_2	1.7%	1.3%	13.4%	2.9%	7.8%	2.3%	15.5%	3.4%	22.4%	15.4%	13.2%	0.4%	0.9%	0.1%
F_3	0.0%	0.7%	8.7%	2.4%	9.0%	2.4%	12.8%	3.6%	22.6%	20.3%	14.3%	1.1%	1.8%	0.3%
F_4	0.0%	0.0%	1.0%	1.9%	5.1%	3.8%	9.1%	4.6%	14.9%	38.0%	17.8%	0.6%	2.8%	0.4%

Relative quantifications based on ^{1}H-^{13}C HSQC spectroscopy measurements. All signals of the defined cross-peaks were summed, corrected for their amount of C-H signals and normalized. Based on this normalized value, the relative abundance of a certain inter-unit linkage or end-group was calculated.

Table S3. ^{31}P-NMR analysis of Parent RCF oligomers (P_1) and its fractions (F_1-F_4).

	C_5 substituted phenols (mmol g^{-1})[a]	Total phenols (mmol g^{-1})[a]	Total aliphatic OH (mmol g^{-1})[a]
P_1	1.78	4.20	2.50
F_1	1.85	3.56	2.89
F_2	2.02	4.04	2.82
F_3	1.89	4.20	2.50
F_4	1.41	4.37	1.87

[a] Quantified by ^{31}P-NMR, spectra can be found in Figure S6-S10.

Table S4. Chemical shifts of the observed oxirane moieties and the two main side-reaction products, measured in $CDCl_3$.

	α (to alcoholic/phenolic oxygen)[a]	β[a]	γ[a]
Aromatic oxirane moiety	70.5 - 4.19 & 70.5 - 4.02	50.2 - 3.37	45.2 - 2.87 & 45.2 - 2.72
Polymerization	71.5 - 4.18	68.8 - 4.38	71.5 - 4.18
Open ring	Overlap with oxirane	71.7 - 4.09	45.6 - 3.87 & 45.6 - 3.74
Aliphatic oxirane moiety	72 - 3.7 & 72. 3.37	51.3 - 3.15	45.1- 2.79 & 45.1 - 2.6

[a] chemical shifts in ^{13}C and ^{1}H dimension measured in $CDCl_3$

Table S5. Optimization of the glycidylation reaction. Approximately 500 mg of lignin was added to a flask together with 20 mol eq. epichlorohydrin (eq. to phenolic content) and 0.1 eq. TBAB. The mixture was stirred and reacted according to the listed conditions.

entry	T 1 (°C)[a]	t 1 (h)[a]	Te 2 (°C)[b]	t 2 (h)[b]	NaOH (eq.)	TBAB (eq.)	Mn (g/mol)[c]	Mw (g/mol)[c]	EEW (g eq^{-1})[d]	S(oxirane on aromatic)[e]	S(open)[e]	S(polymerization)[e]
1	60	3	60	3	3	0.1	630	1069	307	99%	1%	0%
2	85	3	85	3	3	0.1	621	1004	322	80%	20%	0%
3	70	3	70	3	3	0.1	637	1056	294	94%	4%	3%
4	70	3	70	3	5	0.1	647	1103	317	92%	5%	3%
5	60	3	60	3	5	0.1	637	1068	300	97%	2%	1%
6	85	3	25	3	3	0.1	647	1087	358	96%	4%	0%
7	85	5	25	3	3	0.1	633	1166	325	100%	0%	0%

[a] First step of the glycidylation procedure wherein TBAB is mixed with lignin oil and epichlorohydrin. [b] Second step of the glycidylation procedure, NaOH is added dropwise and the reaction continues according to the parameters in the table. [c] determined by GPC of the glycidylated fractions. [d] determined by ^{1}H-NMR. [e] determined by ^{1}H-^{13}C HSQC Spectroscopy

Table S6. Integration results of the glycidylated parent fraction (P_1) and the derived fractions (F_1 to F_4).

	P1	F1	F2	F3	F4
4-Propyl side chain	0.31	0.38	0.27	0.25	0.28
Oxirane moiety on aromatic ring	1	1	1	1	1
Side product 1: Ring Opening	0.01	0	0	0	0
Side product 2: etherifcation - Polymerization	0	0	0	0	0
Oxirane moiety on aliphatic side-chain	0.16	0.24	0.17	0.08	0.01

Table S7. Ratio of 4-propanol/4-propyl of P_1 and F_1-F_4 before and after glycidylation.

	4-propanol/4-propyl ratio[a]	relative decrease of 4-propanol/4-propyl ratio
P_1 before glycidylation	0.63	
P_1 after glycidylation	0.42	33%
F_1 before glycidylation	0.86	
F_1 after glycidylation	0.61	29%
F_2 before glycidylation	0.86	
F_2 after glycidylation	0.59	31%
F_3 before glycidylation	0.70	
F_3 after glycidylation	0.48	32%
F_4 before glycidylation	0.47	
F_4 after glycidylation	0.32	33%

[a] quantified by ^{1}H-^{13}C HSQC spectroscopy

Table S8. Overview of the properties of lignin reported in literature used in lignin-epoxy resin synthesis.

Reference	Lignin type	Mn (g mol^{-1})	DI	Phenolic content (mmol phenol/g)	Aliphatic OH content (aliphatic OH/g)	EEW (g eq^{-1})
[5]	Kraft	1800	3.89	3.29	2.05	442
"	Kraft	2700	4.59	2.79	2.94	614
"	Soda	1900	3.37	2.05	1.80	524
"	Organosolv	1900	2.83	2.20	0.67	343
"	Organosolv	2300	5.00	3.72	1.24	732
"	Organosolv	1750	5.31	1.80	1.26	872
"	Organosolv	1800	4.56	3.08	1.60	481
"	Kraft	2000	4.35	3.41	1.94	546
"	Kraft	1900	3.79	3.04	1.79	438
"	Kraft	1600	2.50	1.90	1.71	374
"	Kraft	1400	2.29	3.78	2.19	359
"	Organosolv	3100	4.94	2.17	2.22	1129
"	Kraft	2000	4.65	3.74	2.37	479
[6]	Kraft	667	1.80	6.80	1.00	256
"	Kraft	1105	1.90	4.70	1.30	313
"	Kraft	1600	2.00	4.40	1.60	323
"	Kraft	2700	2.00	4.50	1.60	370
[17]	Hydrolysis	710	2.99	2.32	2.09	838
[18]	Kraft	1680	1.69	1.40		330
This work	RCF	703	1.40	4.20	2.50	270
This work	RCF	1146	1.55	3.56	2.89	287
This work	RCF	898	1.35	4.04	2.82	291
This work	RCF	662	1.23	4.20	2.50	267
This work	RCF	445	1.22	4.37	1.87	284

5. References

1 X. Meng, C. Crestini, H. Ben, N. Hao, Y. Pu, A. J. Ragauskas and D. S. Argyropoulos, *Nature Protocols*, 2019, **14**, 2627–2647.

2 S. den Bosch, T. Renders, S. Kennis, S.-F. Koelewijn, G. den Bossche, T. Vangeel, A. Deneyer, D. Depuydt, C. M. Courtin, J. M. Thevelein, W. Schutyser and B. F. Sels, *Green Chem.*, 2017, **19**, 3313–3326.

3 T. Renders, G. Van den Bossche, T. Vangeel, K. Van Aelst and B. Sels, *Current Opinion in Biotechnology*, 2019, **56**, 193–201.

4 Y. Jiang, D. Ding, S. Zhao, H. Zhu, H. I. Kenttämaa and M. M. Abu-Omar, *Green Chem.*, 2018, **20**, 1131–1138.

5 S. Nikafshar, J. Wang, K. Dunne, P. Sangthonganotai and M. Nejad, *ChemSusChem*, , DOI:https://doi.org/10.1002/cssc.202002729.

6 C. Gioia, G. Lo Re, M. Lawoko and L. Berglund, *Journal of the American Chemical Society*, 2018, **140**, 4054–4061.

7 C. S. Lancefield, H. L. J. Wienk, R. Boelens, B. M. Weckhuysen and P. C. A. Bruijnincx, *Chem. Sci.*, 2018, **9**, 6348–6360.

8 C. S. Lancefield, S. Constant, P. de Peinder and P. C. A. Bruijnincx, *ChemSusChem*, 2019, **12**, 1139–1146.

9 Y. Wang, X. Meng, K. Jeong, S. Li, G. Leem, K. H. Kim, Y. Pu, A. J. Ragauskas and C. G. Yoo, *ACS Sustainable Chemistry & Engineering*, 2020, **8**, 12542–12553.

10 Y.-Y. Wang, C. E. Wyman, C. M. Cai and A. J. Ragauskas, *ACS Applied Polymer Materials*, 2019, **1**, 1672–1679.

11 S. Constant, H. L. J. Wienk, A. E. Frissen, P. de Peinder, R. Boelens, D. S. van Es, R. J. H. Grisel, B. M. Weckhuysen, W. J. J. Huijgen, R. J. A. Gosselink and P. C. A. Bruijnincx, *Green Chem.*, 2016, **18**, 2651–2665.

12 P. D. Kouris, D. J. G. P. van Osch, G. J. W. Cremers, M. D. Boot and E. J. M. Hensen, *Sustainable Energy Fuels*, 2020, **4**, 6212–6226.

13 P. Paulsen Thoresen, H. Lange, C. Crestini, U. Rova, L. Matsakas and P. Christakopoulos, *ACS Omega*, 2021, **6**, 4374–4385.

14 S. Y. Park, J.-Y. Kim, H. J. Youn and J. W. Choi, *International Journal of Biological Macromolecules*, 2018, **106**, 793–802.

15 X. Meng, S. Bhagia, Y. Wang, Y. Zhou, Y. Pu, J. R. Dunlap, L. Shuai, A. J. Ragauskas and C. G. Yoo, *Industrial Crops and Products*, 2020, **146**, 112144.

16 K. Van Aelst, E. Van Sinay, T. Vangeel, E. Cooreman, G. den Bossche, T. Renders, J. Van Aelst, S. den Bosch and B. F. Sels, *Chem. Sci.*, 2020.

17 F. Ferdosian, Z. Yuan, M. Anderson and C. (Charles) Xu, *Industrial Crops and Products*, 2016, **91**, 295–301.

18 A. Jablonskis, A. Arshanitsa, A. Arnautov, G. Telysheva and D. Evtuguin, *Industrial Crops and Products*, 2018, **112**, 225–235.